Fall Motion Detection Using Combined Range and Doppler Features

Baris Erol and Moeness G. Amin
Center for Advanced Communications
Villanova University
Villanova, PA, 19085, USA
berol@villanova.edu, moeness.amin@villanova.edu

***Abstract*—Feature selection based on combined Doppler and range information improves fall detection and enables better discrimination against similar high Doppler non-rhythmic motions, such as sitting. A fall is typically characterized by an extension in range beyond that associated with sitting, which is determined by the seat horizontal depth. In this paper, we demonstrate, using time-frequency (TF) spectrograms, that range-Doppler radar plays a fundamental and important role in motion classification for assisted living applications. It reduces false alarms along with the associated cost in the unnecessary deployment of the first responders. This reduction is considered vital for the development of in-home radar monitoring and for casting it as a viable technology for aging-in-place.**

I. Introduction

American Association of Retired Persons (AARP) identifies fall detection as a major innovation opportunity to allow seniors to live independently [1]. It is reported that one out of three elderly will fall every year, resulting in injuries and reduced quality of life. Eventually, those with a high risk of falling will move to institutionalized care, which costs roughly $3,500/month. Centers for Disease Control and Prevention (CDC) estimates the direct medical cost of falls to be $34 billion annually [2].

Prompt fall detection saves lives, leads to timely intervention and most effective treatment, and reduces both private and public medical expenses [3]. Fall detection systems also reduce the burden on families that care for senior family members regularly or remotely.

Most researchers divide fall devices into two general types: wearable and non-wearable [4]. The wearable devices are more mature and prevalent. They include accelerometers, push button devices and smartphones, while non-wearable devices include technologies, such as infrared sensors, microphones, pressure sensors, radar, and cameras [5]. The most common non-wearable systems involve cameras. There are, however, several problems with camera systems, as privacy issues are a major concern with elderly users [6]. Further, occlusion and dim lighting are obvious technology limitations. Floor and microphone sensors as well as the others systems remain more in the background as research studies rather than viable commercial solutions.

In this paper, we focus on non-wearable fall detection schemes using radar [7]–[11]. We show improved performance using range-Doppler radar over existing Doppler-only techniques. In general, a robust and smart fall detector is the one that achieves high sensitivity and high specificity. Sensitivity is defined as the ability to correctly classify a fall, i.e., high probability of detection, whereas specificity is the ability to correctly classify a non-fall activity during daily living, i.e., low fall false alarm probability.

Range-Doppler radar systems have clear advantages over Continuous Wave (CW) or Doppler radars in terms of range resolution which is particularly important for indoor human detection. Range estimation for ground and airborne targets and tracking techniques is a mature subject and well-established in the literature [12], [13]. However, the effectiveness of the ultra-wideband (UWB) radar for detection of human motion activities in buildings and inside enclosed structures has not received much attention in the past, especially for the case of fall detection.

The main challenge to radar fall detection is reducing false alarms. One source of false alarms is the possible confusion of fall with sitting and other sudden non-rhythmic motion articulations. The Doppler signatures for the two activities of sitting and falling vary on a case-by-case basis. In many cases, their difference in the TF domain can prove insignificant, depending on how slow or fast each activity is. A situation may arise where the highest Doppler frequency in the two motions assumes close values. In this situation, it has been shown that the radar fall detector, which is only based on Doppler information and employing maximum frequency as a primary feature, suffers from high misclassification rates [14].

In order to avoid mixing falling with sitting, we recognize one subtle difference between these two resembling motions. Unlike falls, the sitting action has limited range extent. This extent is typically determined by the type of the chair and, at most, it is equal to the chair seat horizontal depth. Falls, on the other hand, can extend over a downrange that is equal or longer than the body height. Accordingly, combined range-Doppler information, gained from UWB radar, can be effectively utilized to reduce miss-classification.

The paper is organized as follows. In section II, UWB radar system and the signal model are described. Section III presents three different radar domains, namely, 1) Range-slow time domain, 2) TF domain (Micro-Doppler signatures), 3) Range-Doppler domain. In section IV, experimental setup and

978-0-9928-6265-7/16/$31.00 ©2016 IEEE

description of the database are provided. In section V, feature extraction methods and algorithms based on different radar domains are explained. In section VI, experimental results are provided showing that the proposed fall detection algorithm has superior performance over only Doppler and range-time domain processing. Conclusions are drawn in section VII.

II. UWB Radar System

Extensive data measurements were conducted to demonstrate the contribution of the range-Doppler information for fall detection. The UWB system used in the experiments, named SDR-KIT 2500B, is developed by Ancortek, Inc. This system has built in compact-size, light weight, low-power software defined RF modules and field programmable gate array (FPGA) - based processor module operating in K band (25 GHz). The system offers the ability of integrating transmitter-receiver modules for industry automation, medical monitoring, public safety, security and academic research.

The CW radar is the most commonly used radar type in fall detection. Its main disadvantage is that, without frequency modulation, target range cannot be determined. The CW radar, as such, fails to provide the time difference between the transmit and receive cycles, preventing conversion of time delay to target position.

The employed radar uses linear frequency modulation (LFM) waveforms and is capable of providing both range and Doppler information. LFM waveforms provide a range resolution ΔR,

$$\Delta R = \frac{c}{2\Delta f} \tag{1}$$

where c is the speed of light and Δf is the maximum difference between the modulated signal and the carrier frequency, f_0.

In a frequency modulated continuous-wave (FMCW) radar, both transmitter and receiver ends of the systems are left open for an extended period of time, and this leads to an improved signal-to-noise ratio (SNR). The center frequency of the transmitted signal increases linearly as a function of time over the sweep period, as shown in Fig. 1. The transmitted signal, $s_t(t)$, for the n^{th} sweep can be written as

$$s_t(t) = \sin(2\pi t(f_0 + \frac{\Delta f t}{2})) \tag{2}$$

The received signal, $s_r(t)$, contains valuable information of the moving target which is located at a distance R_T with radial velocity of v. The received signal can be expressed as

$$s_r(t) = a\sin(2\pi(t - t_d)(f_0 + \frac{\Delta f(t - t_d)}{2})) \tag{3}$$

where $t_d = 2R_T/c$ and α is the impact of the target's distance and RCS. Generally, most of the FMCW radar systems employ mixing operation between transmitted and received signals to estimate R_T and v. The mixed signal is passed through a low-pass filter which results in a signal with frequency proportional to the target distance. In this paper, we work with the discrete version of the processed baseband radar return, $s(n)$, i.e.,

$$s(n) = s(t)|_{t=nT_s}, n = 0, 1, \ldots, N-1. \tag{4}$$

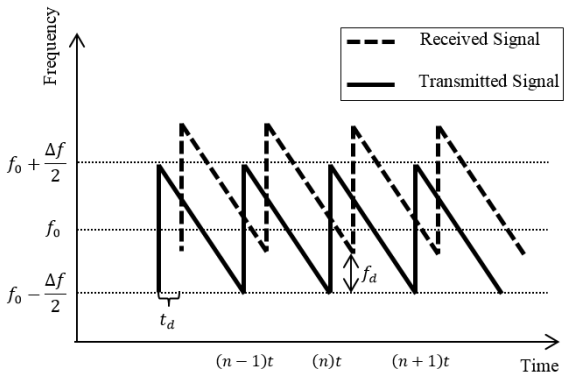

Fig. 1: Transmitted and received LFM signals

where T_s is the sampling period.

III. Tri-Domain Feature Extraction

The received signal, given in (2), is highly non-stationary and contains information about the target's time-dependent range and velocity. This information can be revealed in three different domains, namely, 1) Range-time domain, 2) TF domain (Micro-Doppler signatures), 3) Range-Doppler domain.

A. Range-Slow Time Domain

The received signal can be represented as a two dimensional matrix with each row corresponding to a range bin and each column corresponding to a different pulse, which also represents slow time. To proceed, upon measuring the discrete baseband returned in-phase and quadrature components with a sweep rate $1/T$, we organize the complex data into a two dimensional array. Then, the range profiles of the target can be extracted by applying the Fast Fourier Transform (FFT). Range maps for falling and sitting are shown in Fig. 4-(a) and (d), respectively. A low-pass filter is typically applied in order to remove stationary clutter.

B. Time-Frequency Domain

Micro-Doppler is caused by rotating, oscillating, or vibrating parts of a target, and results in additional frequency modulations centered around the main Doppler shift. The latter is caused by the translational motion of the target [15]. In the case of humans, the complex motions of the limbs, which occur in the course of any motion articulation, result in a micro-Doppler signatures that can be visually distinguishable in the TF domain [16]–[22]. These signatures can be obtained by adding all radar returns over all range bins during the observation period, and then apply a linear or bilinear time-frequency transform of the agglomerate radar range data.

In this paper, we apply short time Fourier transform (STFT) to the slow-time data. The spectrogram $SPEC(n, k)$, which can be interpreted as how the signal power varies with slow time n and Doppler frequency f_d, is the most commonly used time-frequency method for analyzing complex human motions. In this paper, we deal with the radar returns as a

deterministic signal rather than a stochastic process [23]–[25]. The spectrogram can be mathematically expressed as

$$SPEC(n,k) = \left| \sum_{m=0}^{N-1} s(n+m)h(m)e^{-\jmath 2\pi mk/N} \right|^2 \quad (5)$$

where $h(m)$ is a window function that affects both time and frequency resolutions. In this work, spectrograms were generated using 1024 frequency samples, a Hanning window of length 128, and a window overlap of 32 samples. Spectrograms for falling and sitting are given in Fig. 4-(b) and (e), respectively.

C. Range-Doppler Domain

The range-Doppler representation of the radar signal returns is a well-established method that combines both effects of the target velocity and range [26]–[28]. A typical range-Doppler frame is sparse, and contains significant vacant space in both range and Doppler, owing to the small number of targets and short processing interval.

Generally, range-Doppler frame may be constructed by applying Fourier transform over a period of slow time, called coherent processing interval (CPI). A longer CPI duration leads to improved Doppler resolution. The application of the Fourier transform to the range-slow time domain creates a three dimensional data cube, denoted by $I(x, n_{cpi})$, where $x = [f, r]$ corresponds to the range and Doppler coordinates [29]. This process is illustrated in Fig. 2 for fall motion. Range-Doppler processing delivers fairly high resolution in both Doppler and range domains to resolve closely spaced targets with similar velocities. These targets might be non-resolvable by examining range-slow time domain or micro-Doppler signatures separately.

IV. Data Experimental Setup

The UWB radar data sets were collected in the Radar Imaging Lab at the Center for Advanced Communications, Villanova University. An example configuration is depicted in Fig. 3. The UWB radar parameters are: transmitting frequency 24 GHz, the pulse repetition frequency 1000 Hz, bandwidth 2 GHz which provides 0.075 m range resolution, and the total duration for each data collection was determined as 10 seconds.

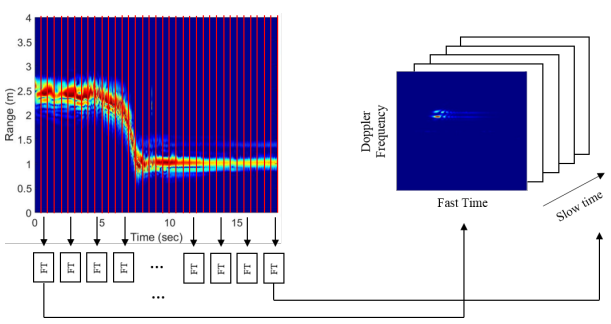

Fig. 2: Traditional range-Doppler processing

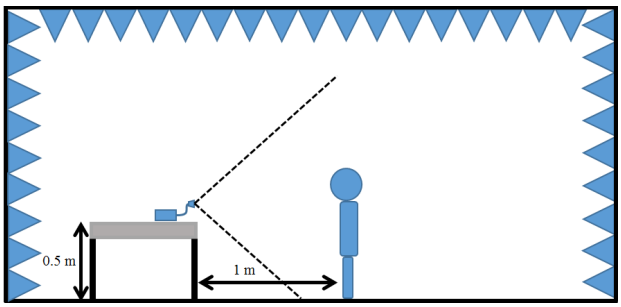

Fig. 3: Schematic of the test configuration

Measurements were made for four different human motion articulations: falling, sitting, bending over, and walking. Each articulation was recorded several times for a duration of 10 seconds, depending on the activity, for 4 subjects, yielding a total of 106 data collections. Out of this number, 40 experiments corresponded to falling and the remaining 66 experiments were related to the three considered non-fall motions. The test subjects posed heights ranging from 1.73 m to 1.90 m, weights ranging from 70 kg to 100 kg, and included 4 males.

V. Fall Detection Algorithms

A. Time-Frequency based Features

Time-frequency characteristics of the radar return contain intrinsic properties about the human motion articulation. As evident from in Fig. 4-(b) and (e), human fall and sit motions have their own unique signatures, which vary depending on speed and kinematics. From these figures, it can be revealed that different joints of the human body have distinguishable signatures. For example, in the case of a fall, human head has the highest Doppler frequency which is formed as an outer envelope in the complete signature, whereas, the Doppler frequency of the lower body is convened densely and compactly in the lower frequency bands. Extracting these important characteristics from the micro-Doppler signature provides, in many but not all cases, discriminative information about the motion.

In this work, three different features were extracted from the spectrograms for fall detection: 1) Extreme (highest) Doppler frequency, 2) Torso frequency, and 3) Length of the event. Details of these feature extraction methods can be found in [30]. An example output of the extreme Doppler frequency at each time instant can be seen in Fig. 4-(b), depicted as red dashed line.

B. Range Spread Feature

Both sitting and falling generate high Doppler frequency components in the TF domain, albeit, falling typically exhibits higher Doppler frequency due to accelerating motion of the body towards to ground. However, slow fall can appear as fast sitting. In this case, and many others, the contribution of the range information becomes important in discriminating motions that have resembling Doppler signatures [31].

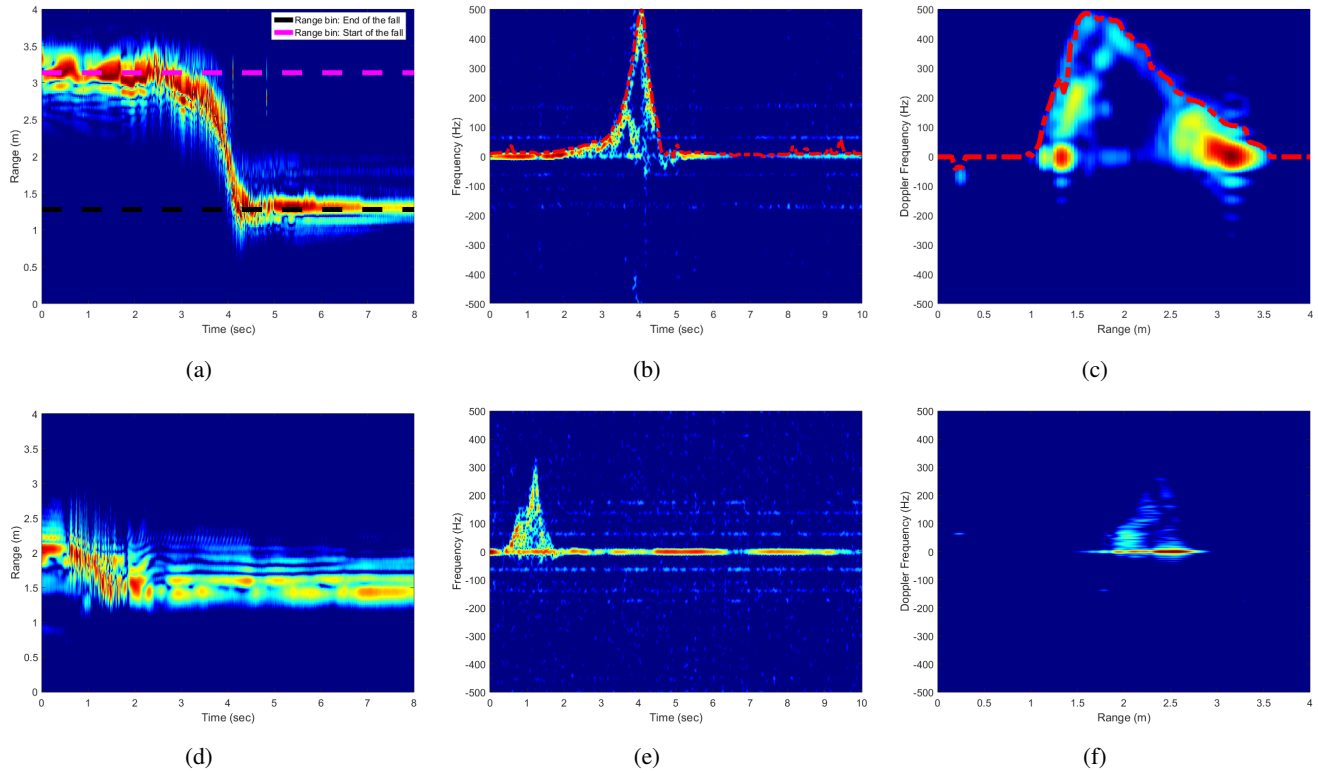

Fig. 4: Tri-domain representations of falling (a) Range-slow time (b) Micro-Doppler signature (c) Time-integrated range-Doppler map and tri-domain representations of sitting (d) Range-slow time (e) Micro-Doppler signature (f) Time-integrated range-Doppler map

To determine the range spread, the range bin which has the most power is first found. This process is repeated for each slow time index, and the entire range vector is constructed. Then, the difference between the minimum and maximum values of the range vector is determined. An example output of the algorithm is depicted in Fig. 4-(a).

C. Combined Range-Doppler Features

Generally, moving target signatures appear as focused and localized in target's range and Doppler away from the origin, whereas stationary targets and clutter are centered around zero Doppler. In this work, we focus on the time-integrated range-Doppler map which is constituted by agglomeration of the consecutive range-Doppler frames [27]. Time-integrated range-Doppler maps have micro-Doppler properties while also providing the range information. Time integrated range-Doppler maps for falling and sitting motions are depicted in Fig. 4-(c) and (f), respectively. We examined three different types of feature sets, namely, PCA-based, correlation-based template matching and integrated range-Doppler motion trajectory to show the offerings of the time-integrated range-Doppler maps in fall detection.

1) PCA-based Features: Most of the proposed radar fall detectors are based on manual-hand picked feature extraction methods which also can be time consuming and highly dependent on parameter tuning and thresholding. In this paper, to establish a baseline performance, we propose an PCA-based fall detection approach [32]. The time integrated range-Doppler maps are processed as grayscale images and used as inputs to the eigen decomposition. The PCA-based approach has similar steps to those typically employed in face recognition [33]. The training involves the following initialization operations for each sample:

1) Acquire a initial set of grayscale time integrated range-Doppler images
2) Compute the eigenimages from each training image, keeping only the 5 images that correspond to the highest eigenvalues.

Employing the initialized training system, the following steps can then be used to recognize new samples:

1) Compute a set of weights based on the input test sample and 5 eigenimages.
2) Determine the class of the test sample by using minimum Euclidean distance to find the closest match in the training data.

2) Correlation-based Template Matching Features: The second approach for fall detection consists of a correlation-based template matching algorithm [26]. It is generally applied to consecutive range-Doppler frames, but we only apply it, in context of motion detection, to the time integrated

TABLE I: Scores (%) for each feature set by six different metrics

	Accuracy	Sensitivity	Specificity	Fall detection rate	False alarm rate	Missed rate
TF-based	91.98	94.93	89.39	88.70	4.73	11.3
TF-based + range spread	95.27	93.45	95.22	95.20	6.67	4.78
Range-Doppler: PCA-based	92.18	95.15	89.58	88.90	4.53	11.10
Range-Doppler: Correlation-based	98.00	99.77	96.35	96.20	0.22	0.41
Range-Doppler: Integrated motion trajectory	99.60	99.62	99.59	99.60	0.37	0.41

range-Doppler images. The correlation between two different grayscale images can be defined as

$$c_{cor} = \frac{\sum_{r=0}^{r_m} \sum_{f=-f_s/2}^{f_s/2} P_1(r,f)P_2(r,f)}{\sqrt{\sum_{r=0}^{r_m} \sum_{f=-f_s/2}^{f_s/2} P_1^2(r,f)} \sqrt{\sum_{r=0}^{r_m} \sum_{f=-f_s/2}^{f_s/2} P_2^2(r,f)}} \quad (6)$$

where f_s is the sampling frequency, P_1 and P_2 are the different gray-scale time integrated range-Doppler images, and r_m is the maximum range, which in our case is 8 meters.

The training and testing schemes are similar to the PCA approach. After the training set is constructed, correlation between test and each training image is computed. Test image is classified as the label of the training image which provides the highest correlation. An example of a correlation map is depicted in Fig. 5. It is evident that the fall and non-fall classes of motions have their unique regions, albeit, it is also noticed that some of the fall and non-fall samples have high correlation. The latter is caused by the similarity between slow falling and fast sitting motions. This confusion is expected considering that the algorithm still depends on the Doppler information.

3) Integrated Range-Doppler Features: This approach is designed to take advantage of the target trajectory information in both range and Doppler. An example of the range-Doppler trajectory of a fall is depicted as dashed red line in Fig. 4-(c). Since different motions manifest their unique characteristic

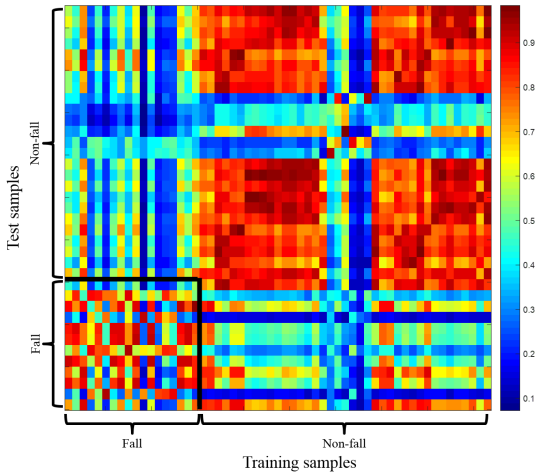

Fig. 5: Correlation map between training and test samples

based on the motion boundaries or trajectories in the range-slow time domain and in the TF domain, we also seek to determine the motion trajectory in the time integrated range-Doppler maps.

An energy-based thresholding algorithm is established to determine the trajectory of the integrated time range-Doppler map. First, the energy in the range bin r is computed as

$$E_R(r) = \sum_{k=1}^{M} P(r,k) \quad (7)$$

where $k = 1, 2, ..., M$ are the Doppler indices. Next, for the range index r, the first frequency bin whose corresponding range-Doppler value is greater than or equal to the product of a pre-determined threshold and E_R is determined. The two-step process is repeated for all $r = 1, 2, ..., N$, leading to extraction of the motion trajectory.

VI. Experimental Results

The five aforementioned feature sets were extracted for comparison. A support vector machine (SVM) classifier with a radial basis kernel function was used for TF-based, range spread, integrated range-Doppler motion trajectory feature sets. On the other hand, Euclidean distance classifier was employed for both correlation-based template matching and PCA-based feature sets. 60% of the recorded signals were used for training the classifier, whereas the remaining 40% were used as testing. Training and test samples were selected in a random fashion to utilize the classifiers in a better manner. Therefore, 1000 Monte Carlo trials were conducted to eliminate the random selection effect on classification results.

We use a variety of performance criteria to evaluate the different feature extraction methods. The first metric, accuracy, is the proportion of the total number of fall and non-fall predictions that are correctly classified. Accuracy, however, is not a reliable metric to determine the real performance of the system in which the training data set is unbalanced. The second metric, sensitivity, measures the proportion of the correctly classified falls, whereas specificity computes the proportion of non-falls which are correctly identified. Fall detection, false alarm and missed rates are commonly used performance metrics which can also be exploited by examining the confusion matrix.

Table 1 shows the score for each feature extraction algorithm on each of the six metrics. TF-based features provide a fairly high performance on sensitivity metric but fails to provide low missed rate because of the similarity between slow

falling and fast sitting micro-Doppler signatures. The case where the TF-based and range spread features are employed together, missed rate is decreased to a level of 4.78% but still there is a little confusion between walking and falling motions due to the similar range spread values. Range-Doppler domain PCA-based features fail to yield good classification results, whereas both correlation-based template matching and motion trajectory features yield high classification performances. Among the range-Doppler algorithms, motion trajectory features produce the highest accuracy, sensitivity, specificity and fall detection rates. The lowest missed rate is provided by both template-based and motion trajectory features at a level of 0.41%, whereas template-based features provide the lowest fall alarm rate.

VII. Conclusion

In this paper, we have applied range-Doppler domain feature extraction methods for radar-based fall motion detection. Real data measurements were collected corresponding to four different motions: falling, sitting, picking up an object and walking. The employed range-Doppler domain feature extraction methods were PCA-based, correlation-based template matching and target trajectory information. Experimental results were provided which demonstrated the superiority of the range-Doppler domain-based features over the conventional TF-based and range spread features in correctly between fall and non-fall classes.

Acknowledgments

This paper is made possible by NPRP Grant # NPRP 6-680-2-282 from the Qatar National Research Fund (a member of Qatar Foundation). The statements made herein are solely the responsibility of the authors.

References

[1] *Health Innovation Frontiers: Untapped Market Opportunities for the 50+*. http://www.aarp.org/content/dam/aarp/home-and-family/personal-technology/2013-08/Health-Innovation-Frontiers-Untapped-Market-Opportunities-for-50%2B-Full-Report-AARP.pdf., 2013.

[2] *Center for Diease Control and Prevention, Important facts about falls*. http://www.cdc.gov/homeandrecreationalsafety/falls/adultfalls.html., 2015.

[3] L. Z. Rubenstein and K. R. Josephson, "The epidemiology of falls and syncope," *Clin. Geriatr. Med.*, vol. 18, no. 2, pp. 141–158, 2002.

[4] F. Ahmad, A. E. Cetin, K. C. Ho, and J. E. Nelson, "Special section on signal processing for assisted living," *IEEE Sig. Process. Mag.*, vol. 33, no. 2, pp. 25–94, 2016.

[5] R. Igual, C. Medrano, and I. Plaza, "Challenges, issues and trends in fall detection systems," *Biomed Eng Online*, vol. 12, no. 66, p. 66, 2013.

[6] F. Bagala, C. Becker, A. Cappello, L. Chiari, K. Aminian, J. M. Hausdorff, W. Zijlstra, and J. Kenk, "Evaluation of accelerometer-based fall detection algorithms on real-world falls," *PLos ONE*, vol. 7, no. 5, 2012.

[7] Q. Wu, Y. D. Zhang, W. Tao, and M. G. Amin, "Radar-based fall detection based on doppler time-frequency signatures for assisted living," *Sonar Navigation IET Radar*, vol. 9, no. 2, pp. 164–172, 2015.

[8] L. Liu, M. Popescuand, M. Skubicand, M. Rantzand, T. Yardibi, and P. Cuddihy, "Automatic fall detection based on doppler radar motion signature," *in 2011 5th International Conference on Pervasive Computing Technologies for Healthcare (PervasiveHealth)*, pp. 222–225, 2011.

[9] B. Y. Su, K. C. Ho, M. J. Rantz, and M. Skubic, "Doppler radar fall activity detection using the wavelet transform," *IEEE Transactions on Biomedical Engineering*, vol. 62, no. 3, pp. 865–875, 2015.

[10] J. Hong, S. Tomii, and T. Ohtsuki, "Cooperative fall detection using doppler radar and array sensor," *in 2013 IEEE 24th International Symposium on Personal Indoor and Mobile Radio Communications*, pp. 3492–3496, 2013.

[11] M. G. Amin, Y. D. Zhang, F. Ahmad, and K. C. Ho, "Radar signal processing for elderly fall detection: The future for in-home monitoring," *IEEE Signal Processing Magazine*, vol. 33, no. 2, pp. 71–80, 2016.

[12] J. F. Dickey, M. Labitt, and F. M. Staudaher, "Development of airborne moving target radar for long range surveillance," *IEEE Transaction on Aerospace and Electronic Systems*, vol. 27, no. 6, pp. 959–972.

[13] J. Li, G. Liu, N. Jiang, and P. Stoica, "Moving target feature extraction for airborne high-range resolution phased-array radar," *IEEE Transaction on Signal Processing*, vol. 49, no. 2, pp. 227–289.

[14] F. Ahmad, R. M. Narayanan, and D. Schreurs, "Special issue on application of radar to remote patient monitoring and eldercare," *IET Radar, Sonar, and Navig.*, vol. 9, no. 2, pp. 115–190, 2015.

[15] V. C. Chen, *The micro-Doppler effect in radar*. Artech House, 2011.

[16] Y. Kim and H. Ling, "Human activity classification based on micro-doppler signatures using a support vector machine," *IEEE Transactions on Geoscience Remote Sensing*, vol. 47, no. 5, pp. 1328–1337, 2009.

[17] P. V. Dorp and F. C. A. Groen, "Feature-based human motion parameter estimation with radar," *Sonar Navigation IET Radar*, vol. 2, no. 2, pp. 135–145, 2008.

[18] Y. Kim, S. Ha, and J. Kwon, "Human detection using doppler radar based on physical characteristics of targets," *IEEE Geoscience and Remote Sensing Letters*, vol. 12, no. 2, pp. 289–293, 2015.

[19] B. G. Mobasseri and M. G. Amin, "A time-frequency classifier for human gait recognition," *Proc. SPIE*, vol. 73062, 2009.

[20] C. Karabacak, S. Z. Gurbuz, A. C. Gurbuz, M. B. Guldogan, G. Hendeby, and F. Gustafsson, "Knowledge exploitation for human micro-doppler classification," *IEEE Geoscience and Remote Sensing Letters*, vol. 12, no. 10, pp. 2125–2129, 2015.

[21] I. Orovic, S. Stankovic, and M. Amin, "A new approach for classification of human gait based on time-frequency feature representations," *Signal Processing*, vol. 91, no. 6, pp. 1448–1456.

[22] M. Otero, "Application of a continuous wave radar for human gait recognition," *Proceedings of SPIE Signal Processing, Sensor Fusion, and Target Recognition XIV*, vol. 5809, 2005.

[23] W. Martin and P. Flandrin, "Wigner-ville spectral analysis of nonstationary processes," *IEEE Trans. Acoust., Speech, Signal Process.*, vol. 33, no. 6, p. 14611470, 1985.

[24] M. G. Amin, "Minimum variance time-frequency distribution kernels for signal in additive noise," *IEEE Transactions on Signal Processing*, vol. 44, pp. 2352–2356, 1996.

[25] M. G. Amin, "Time-frequency spectrum analysis and estimation for nonstationary random processes," in *Time-Frequency Signal Analysis: Methods and Applications* (B. Boashash, ed.), Longman Cheshire, 1992.

[26] S. Fukushima, H. Yamada, H. Kobayashi, and Y. Yamaguchi, "Human motion detection and extraction by using fm-cw range-doppler radar," *2014 International Symposium on Antennas and Propagation (ISAP)*, pp. 173–174.

[27] D. Tahmoush and J. Silvious, "Time-integrated range-doppler maps for visualizing and classifying radar data," *2011 IEEE Radar Conference (RADAR)*, pp. 372–374.

[28] Y. He, P. Molchanov, T. Sakamoto, P. Aubry, F. L. Chevalier, and A. Yarovoy, "Range-doppler surface: a tool to analyse human target in ultra-wideband radar," *Sonar Navigation IET Radar*, vol. 9, no. 9, pp. 1240–1250.

[29] O. R. Fogle and B. D. Rigling, "Micro-range/micro-doppler decomposition of human radar signatures," *IEEE Transactions on Aerospace and Electronic Systems,*, pp. 3058–3072, 2012.

[30] B. Erol, M. G. Amin, F. Ahmad, and B. Boashash, "Radar fall detectors: A comparison," *Proceedings of SPIE Radar Sensor Technology XX*, vol. 9829, 2016.

[31] B. Erol, M. G. Amin, Z. Zhou, and J. Zhang, "Range information for reducing fall false alarms in assisted living," *2016 IEEE Radar Conference (RADAR)*, 2016.

[32] B. Jokanovic, M. G. Amin, F. Ahmad, and B. Boashash, "Radar fall detection using principal component analysis," *Proceedings of SPIE Radar Sensor Technology XX*, vol. 9829, 2016.

[33] M. Turk and A. Pentland, "Eigenfaces for recognition," *J. cognitive neuroscience*, vol. 3, no. 61, pp. 71–86.